

Thermal behavior of metal nanoparticles in geologic materials

Martin Reich*

Department of Geological Sciences, University of Michigan, Ann Arbor, Michigan 48109-1005, USA, and
Departamento de Geología, Facultad de Ciencias Físicas y Matemáticas, Universidad de Chile, Santiago, Chile

Satoshi Utsunomiya

Stephen E. Kesler

Department of Geological Sciences, University of Michigan, Ann Arbor, Michigan 48109-1005, USA

Lumin Wang

Department of Nuclear Engineering and Radiological Sciences, University of Michigan, Ann Arbor, Michigan 48109-2104, USA

Rodney C. Ewing

Udo Becker

Department of Geological Sciences, University of Michigan, Ann Arbor, Michigan 48109-1005, USA

ABSTRACT

Although significant progress has been made in understanding the behavior of natural nanoparticles in Earth's critical zone (i.e., surface and near-surface environment), little is known about nanoparticle stability in higher-temperature environments where they are increasingly being found. Here we report the first direct observations of the thermal behavior of natural nanoparticles at near atomic scale, revealing that their thermal stability is dependent on particle size and on the surrounding host mineral. Native Au nanoparticles (mean diameter ~4 nm) incorporated in arsenian pyrite from refractory Au ores were observed under the transmission electron microscope during in situ heating to 650 °C. While isolated Au nanoparticles melt, with the melting point being a function of size, we show that when incorporated in arsenian pyrite, Au nanoparticles become unstable unless the nanoparticle size distribution coarsens by diffusion-driven, solid-state Ostwald ripening. This change in nanoparticle stability starts above 370 °C, setting an upper temperature and size limit for the occurrence of nanoparticulate Au in refractory sulfides. These findings not only provide new insights into the behavior of nanoparticulate Au and other metals during geological processes and throughout their metallurgical recovery from refractory ores, but also provide a new tool to define the thermal history of nanoparticle-bearing geologic and planetary materials.

Keywords: nanoparticles, gold, Ostwald ripening, Carlin-type gold, epithermal.

INTRODUCTION

Natural nanoparticles are attracting attention due to their unique role as agents of elemental transport and their increased reactivity in geologic systems (Hochella, 2002a, 2002b). The occurrence of native metal, oxide, sulfide, and silicate nanoparticles has been documented in a variety of low-temperature natural materials such as soils, sediments, and atmospheric aerosols, as well as in higher-temperature materials, including metal sulfide ores and meteorites (Lewis et al., 1987; Saunders, 1990; Anastasio and Martin, 2001; Palenik et al., 2004; Hochella et al., 2005; Waychunas et al., 2005). The behavior of mineral nanoparticles in natural systems is still not well understood due to a lack of experimental evidence about their physico-chemical properties. Although it is known that a decrease in particle size to the nanoscale level can promote phase instability due to the increase in surface energy (Halperin, 1986; McHale et al., 1997; Navrotsky, 2001), information is needed on how nanoscale effects affect the occurrence of nanoparticles at temperatures typical of near-surface to deep-crustal conditions. We report here observations on the thermal stability of nanoparticles of native Au in refractory sulfides that provide important new insights into the conditions that limit the formation of nanoparticles in high-temperature geological materials.

SAMPLES AND METHODS

Our observations were made on Au nanoparticles (AuNPs) in arsenian pyrite [Fe(S,As)₂], a mineral that is widespread in sediments, sedimentary rocks, and hydrothermal ore deposits that formed at temperatures as high as 350 °C. Arsenian pyrite is particularly abundant in Carlin-type and epithermal gold deposits (Hofstra and Cline, 2000; Cooke and Simmons, 2000), where it is an important host for Au, much of which is invisible to conventional microscopy. Reich et al. (2005a) showed that Au speciation in arsenian pyrite is controlled by the Au/As molar ratio, Au⁺¹ (solid-solution Au) being the dominant species for Au/As < 0.02. When this solubility limit is exceeded, nanoparticulate Au⁰ occurs, and geologic and mineralogical evidence suggests that these nanoparticles precipitate from slightly supersaturated hydrothermal solutions at temperatures below 250 °C (Reich et al., 2005a).

In order to test the stability of AuNPs as a function of temperature and particle size, in situ heating experiments were carried out on arsenian pyrite samples from Carlin-type deposits in Nevada. The analyzed samples contain highly dispersed native AuNPs having an average size of ~4 nm (bright spots in Fig. 1A). Secondary ion mass spectrometry analysis and electron probe microanalysis of these pyrites reveal that Au (total ~8000 ppm) is contained in both Au⁰ (nanoparticles) and Au⁺¹ (solid solution) (Reich et al., 2005a). Arsenian pyrite grains were cut ultrasonically from 30 μm polished thin sections, mounted on 3 mm Cu grids, and milled with an Ar ion beam (4.0 keV, <30 min/sample). Samples were placed on a regular double-tilt heating

*E-mail: mreichm@umich.edu.

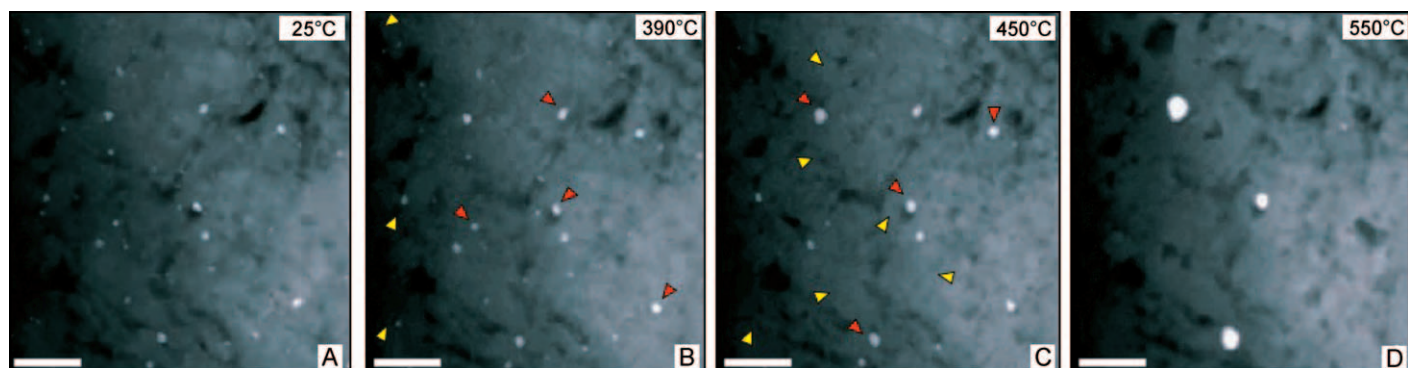


Figure 1. Ostwald ripening of Au nanoparticles (AuNPs) in arsenian pyrite. High-angle annular dark field detector with scanning transmission electron microscopy images show no visible changes from 25 °C (A) until ~390 °C (B), where smaller AuNPs dissolve and larger ones start to coarsen. At 450 °C (C), larger particles have grown at expenses of smaller ones. At 550 °C (D), only three particles of >20 nm diameter survive in view of 0.2 μm^2 (Video DR1 [see footnote 1]). Yellow arrows indicate particles that have dissolved with respect to previous frame, and red arrows show particles that have coarsened with respect to previous temperature step. Scale bar is 100 nm.

holder connected to a Gatan Smart Set Model 901 Hot Stage Controller, which allows controlled heating of the sample between 25 °C and ~800 °C. Temperature was raised manually during observation. In situ examination was carried out using high-resolution transmission electron microscopy (HRTEM) coupled with a high-angle annular dark field detector with scanning transmission electron microscopy

(HAADF-STEM) that allows average atomic mass (Z) contrast imaging at nanoscale (Utsunomiya and Ewing, 2003). Sample changes during heating were recorded live using a digital image capture system, and image processing, including Fast Fourier Transformation and particle size analysis, was completed using Gatan Digital Micrograph 3.4. No sample alteration due to electron beam irradiation was noted during TEM examination (sample irradiation tests were undertaken according to Palenik et al., 2004).

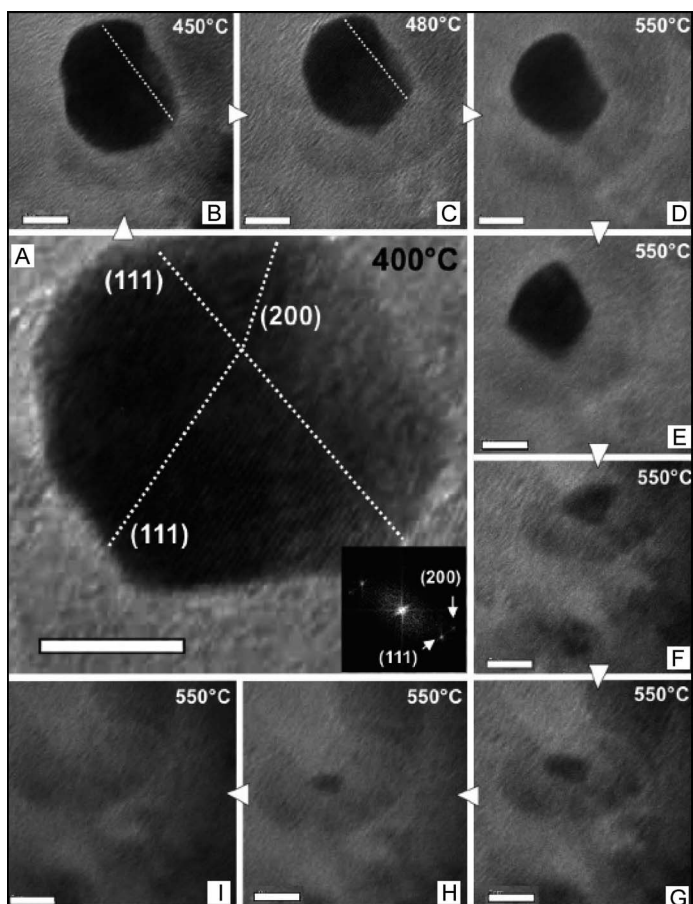


Figure 2. Dissolution of single Au nanoparticle (AuNP) into its pyrite host. Selected high-resolution transmission electron microscopy (HRTEM) images show evolution of single AuNP during heating starting at 400 °C (A). Size and/or shape changes start at ~450 °C (B, C) (Videos DR2 and DR3 [see footnote 1]), although most significant decrease in size occurs at 550 °C (D–H), until final dissolution (I) (Video DR4). Scale bar is 5 nm and inset in A is Fast Fourier Transform (diffraction pattern) of HRTEM image of AuNP.

IN SITU TEM HEATING EXPERIMENTS

In situ HAADF-STEM observations show that AuNPs (bright spots on the darker arsenian pyrite matrix) remained unchanged from room temperature (Fig. 1A) to ~370 °C, where the smallest Au particles (<2 nm) start to dissolve into the pyrite matrix (Data Repository Video DR1¹). At 390 °C (Fig. 1B), coarsening of some larger particles (~8 nm) is noticeable, although the most evident changes in nanoparticle size and distribution are observed above 400 °C. Above this temperature, larger AuNPs grow at the expense of the smaller ones (Fig. 1C). AuNPs remain immobile during heating and no coalescence (where two larger particles combine) is observed. At 550 °C, the upper temperature limit of this heating experiment, only 3 nanoparticles (~30–35 nm) survive in the area of observation, replacing the initial 115 of average size ~4 nm (Fig. 1D; Video DR1). It is likely that further heating would have caused these three particles to merge into a single larger one, although this could not be confirmed because of technical limits of the heating system. Upon cooling from 550 °C to room temperature, these larger particles remain unchanged, indicating that coarsening of Au nanoparticles is irreversible. The discrepancy between the Au budgets of large particles with respect to the small particles from which they grew (i.e., more Au contained in the larger particles than in the initial small particle distribution) is the result of solid-solution Au remobilization during the heating experiment.

Insight into the mechanism by which the nanoparticles dissolve into pyrite is obtained using HRTEM on a faceted ~15 nm AuNP with a pronounced crystallographic relationship between particle faces and host mineral (Fig. 2A). During heating this AuNP shows no apparent variations in size or shape until ~440–450 °C, when it starts to decrease in size and crystal facets become irregular (Fig. 2B; Video DR2). Between 480 and 550 °C, the AuNP continues to shrink, and its edges are no longer aligned parallel to specific crystallographic di-

¹GSA Data Repository item 2006225, Videos DR1–DR5, videos of in situ transmission electron microscopy heating experiments showing dissolution and growth of Au nanoparticles at near-atomic scale, is available online at www.geosociety.org/pubs/ft2006.htm, or on request from editing@geosociety.org or Documents Secretary, GSA, P.O. Box 9140, Boulder, CO 80301, USA.

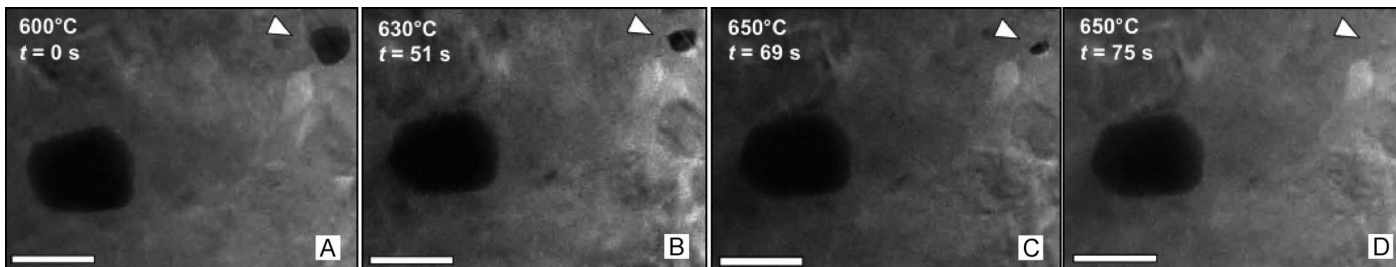


Figure 3. Sequence of selected high-resolution transmission electron microscopy images during heating of two Au nanoparticles (AuNPs) of different sizes (~50 and 25 nm). Starting at 600 °C (A), smaller AuNP progressively decreases in size (B, C) until it dissolves at 650 °C, 75 s (t is time) after initiation of experiment (Video DR5 [see footnote 1]). Scale bar is 50 nm. Arrows indicate dissolving AuNP.

rections (Figs. 2C, 2D; Video DR3). At 550 °C, it is dramatically reduced in size (Figs. 2D–2H) and finally dissolves completely (Fig. 2I; Video DR4). When two AuNPs of different sizes (~50 nm and ~25 nm) in close proximity are heated above 600 °C (under HRTEM mode), the smaller AuNP progressively decreases in size with increasing temperature until it disappears completely at 650 °C (Figs. 3A–3D; Video DR5).

THERMAL STABILITY OF Au NANOPARTICLES

It is well known that the melting temperature of bulk Au (1064 °C) decreases significantly when particle dimensions are reduced to the nanoscale. Therefore, an ~3-nm-diameter Au particle can melt at temperatures as low as ~500 °C, due to the increase in the surface/volume ratio (Buffat and Borel, 1976; Ercolessi et al., 1991; Lewis et al., 1997). However, our particle size versus temperature data show that larger AuNPs grow at the expense of the smaller ones in a solid-state, Ostwald-type ripening process (Fig. 4, lower curve) before they reach the size-dependent melting points of isolated AuNPs (Fig. 4, upper curve).

The lower (coarsening) curve in Figure 4 sets an upper tempera-

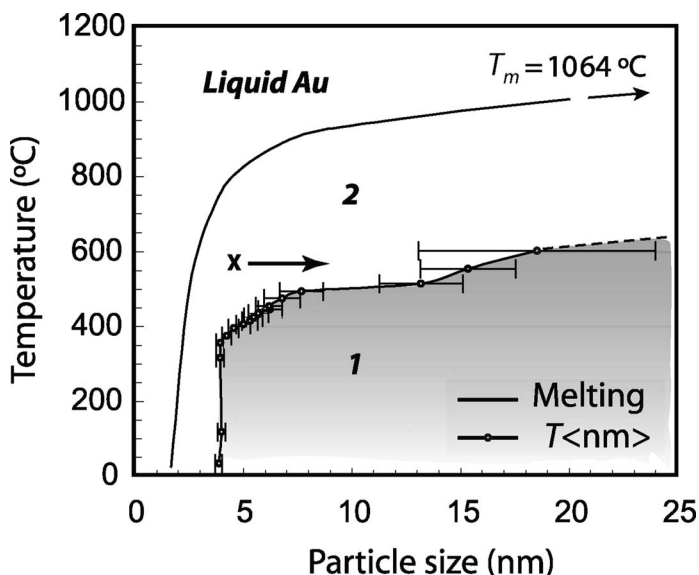


Figure 4. Stability of Au nanoparticles (AuNPs) as function of temperature (T), particle size, and host material. Dark gray lower field (1), limited above by experimental coarsening curve (bars represent particle size distribution), defines stability range of AuNPs in arsenian pyrite host. Above this upper temperature limit (e.g., point x), AuNPs in pyrite are unstable unless coarsening occurs (arrow direction). However, AuNPs in isolation (from solid host) are stable within field 2 (which partially overlaps field 1), until they reach upper melting curve (data from Buffat and Borel, 1976; T_m = melting point of bulk Au).

ture limit for the stability field of AuNPs in arsenian pyrite (field 1, dark gray). At any temperature above this limit (field 2), AuNPs will not be stable unless coarsening occurs (see arrow direction in Fig. 4). The difference between the melting temperature of isolated AuNPs (upper curve) and the temperature at which complete dissolution of AuNPs into the surrounding pyrite occurs (lower curve) is influenced by (1) the energy gain due to dissolution of AuNPs into the surrounding matrix, (2) the energy loss of disrupting the former AuNP-host interface, and (3) the loss of intra-AuNP interactions. Even though we cannot make a clear distinction between these contributing factors using the measurements presented in this paper, we can say that the energy gain due to dissolution (1) outweighs the energy-loss contributions of 2 and 3. The stability of AuNPs as a function of size and temperature, as shown here, not only reflects the thermo-physical properties of the AuNPs, but also the physico-chemistry of the AuNP-host interaction. A few studies have suggested that the nature of the nanoparticle surroundings can have a profound impact on nanoparticle stability (Zhang et al., 2003; Gilbert et al., 2004). From the particle size-temperature data in Figure 4, we conclude that the surrounding sulfide host plays an important role in promoting solid-state dissolution of AuNPs before a solid→liquid phase transition occurs.

Results from our heating experiments provide a constraint on the upper temperature limit of the stability of AuNPs in arsenian pyrite and valuable information on the nature of the physico-chemical processes operating during heating. Two distinctive features are observed during the dissolution of AuNPs: (1) the faster disappearance of the (100) Au faces [apparent as (200) diffraction maxima in Fig. 2A] than the (111) faces as the Au nanoparticle shrinks (Figs. 2A–2C) and (2) the development of a dark-contrast halo around the AuNP (Figs. 2B–2H). Both observations document the important role of diffusion during heating of AuNPs. Molecular dynamics simulations on pyrite-encapsulated Au clusters show that (111) faces are more stable than (100) faces upon heating (Reich et al., 2005b), consistent with previous reports on isolated AuNPs (Carnevali et al., 1987). Thus, the preferential detachment of Au atoms from (100) faces over (111) faces, followed by diffusion throughout the matrix and reattachment to larger particles, accounts for the observed changes in nanoparticle shape and size during heating experiments (Figs. 1–3). This interpretation is supported by the presence of dark halos of diffraction contrast that develop around the AuNP upon heating (Figs. 2B–2H) that may be the result of highly concentrated Au atoms dissolved in the pyrite matrix or pyrite lattice strain effects, as reported for Fe⁰ nanoparticles in Al₂O₃ (Fei et al., 2002).

CONSTRAINTS ON THE NATURAL OCCURRENCE OF NANOPARTICULATE METALS

Naturally formed nanoparticles are subject to size and host effects that alter their thermal stability and, therefore, their occurrence in the geologic record. Our observations reveal that AuNPs in arsenian pyrite remain stable until they start to coarsen into larger particles above

~370 °C. Hence, our observations set a constraint on the upper temperature limit of occurrence of AuNPs in arsenian pyrite in hydrothermal systems, a result that agrees with empirical evidence about the distribution of nanoparticulate Au in hydrothermal Au deposits (Mumin et al., 1994; Cooke and Simmons, 2000; Palenik et al., 2004). Although the empirical coarsening curve in Figure 4 defines an upper limit for nanoscale Au stability (under experimental TEM observation), its dependence on other variables such as heating rate, pressure, As content of pyrite, and diffusion time scale has to be evaluated in future studies.

For any AuNP-bearing mineral, the position of the coarsening curve of AuNPs in temperature-particle size space will depend on the solubility of Au within its host. Therefore, as a first approximation, the coarsening curve in Figure 4 will shift upward if AuNPs are incorporated in a mineral host where Au is less soluble than arsenian pyrite. In the limiting case, if Au is insoluble in a certain mineral host (e.g., Au in a silicate phase), AuNPs will respond to increased temperature by melting instead of coarsening. However, AuNPs will easily dissolve within host phases such as, e.g., Ag-Cu alloys, where Au miscibility is high. In this case, the coarsening curve will shift downward.

Our results show that nanoparticulate metals, usually thought to be prevalent in low-temperature ($T < 100$ °C) aqueous environments, can also occur and remain stable at higher temperatures in well-defined temperature-particle size limits. Independent of the nature of the nanoparticle-host system studied, the methodology presented here is a novel tool to evaluate the thermal history of nanoparticle-bearing geologic materials. As the mean particle size of a particular nanoparticle distribution sets an upper limit of stability, T versus particle size (nm) stability diagrams can be used to estimate the maximum temperature of the host rock.

In addition, these observations may also have an impact on the metallurgical recovery of Au and other noble metals in refractory sulfide ores. AuNPs constitute a significant fraction of the invisible Au in refractory pyrite and arsenopyrite in these ores. Currently, refractory Au ores are oxidized first in order to render the Au accessible to chemical leach (La Brooy et al., 1994). A better understanding of the temperature behavior of the nanoparticulate Au encapsulated in the refractory sulfides during pressure (~170–225 °C) or oxidizing roasting (~650–700 °C) may lead to more cost-effective methods for metal recovery.

ACKNOWLEDGMENTS

We acknowledge the support of this study by the National Science Foundation Nanoscale Interdisciplinary Research Team program (grant EAR-0403732). Reich and Utsunomiya thank John Mansfield for his support in the Electron Microbeam Analysis Laboratory at the University of Michigan. Reich also acknowledges scholarship support from Fulbright-Mecsup programs. We thank Alexandra Navrotsky and two anonymous reviewers for their insightful comments and suggestions.

REFERENCES CITED

Anastasio, C., and Martin, S.T., 2001, Atmospheric nanoparticles: Reviews in Mineralogy and Geochemistry, v. 44, p. 293–349.
 Buffat, P., and Borel, J.P., 1976, Size effect on the melting temperature of Au particles: *Physical Review A*, v. 13, p. 2287–2298, doi: 10.1103/PhysRevA.13.2287.
 Carnevali, P., Ercolessi, F., and Tosatti, E., 1987, Melting and nonmelting behavior of the Au (111) surface: *Physical Review B: Condensed Matter and Materials Physics*, v. 36, p. 6701–6704.
 Cooke, D.R., and Simmons, S.F., 2000, Characteristics and genesis of epithermal Au deposits: *Reviews in Economic Geology*, v. 13, p. 221–244.
 Ercolessi, F., Andreoni, W., and Tosatti, E., 1991, Melting of small Au particles:

Mechanism and size effects: *Physical Review Letters*, v. 66, p. 911–914, doi: 10.1103/PhysRevLett.66.911.
 Fei, G.T., Barnes, J.P., Petford-Long, A.K., Doole, R.C., Serna, R., and Gonzalo, J., 2002, Structure and thermal stability of Fe:Al₂O₃ nanocomposite films: *Journal of Physics D-Applied Physics*, v. 35, p. 916–922, doi: 10.1088/0022-3727/35/9/313.
 Gilbert, B., Huang, F., Zhang, H., and Banfield, J.F., 2004, Nanoparticles: Strained and stiff: *Science*, v. 305, p. 651–654.
 Halperin, W.P., 1986, Quantum size effects in metal particles: *Reviews of Modern Physics*, v. 58, p. 533–606, doi: 10.1103/RevModPhys.58.533.
 Hochella, M.F., 2002a, Nanoscience and technology: The next revolution in the Earth sciences: *Earth and Planetary Science Letters*, v. 203, p. 593–605, doi: 10.1016/S0012-821X(02)00818-X.
 Hochella, M.F., 2002b, There's plenty of room at the bottom: *Nanoscience in geochemistry: Geochimica et Cosmochimica Acta*, v. 66, p. 735–743, doi: 10.1016/S0016-7037(01)00868-7.
 Hochella, M.F., Jr., Moore, J.N., Putnis, C.V., Putnis, A., Kasama, T., and Eberl, D.D., 2005, Direct observation of heavy metal-mineral association from the Clark Fork River Superfund Complex: Implications for metal transport and bioavailability: *Geochimica et Cosmochimica Acta*, v. 69, p. 1651–1663, doi: 10.1016/j.gca.2004.07.038.
 Hofstra, A.H., and Cline, J.S., 2000, Characteristics and models for Carlin-type Au deposits: *Reviews in Economic Geology*, v. 13, p. 163–220.
 La Brooy, S.R., Linge, H.G., and Walter, G.S., 1994, Review of Au extraction from ores: *Minerals Engineering*, v. 7, p. 1213–1241, doi: 10.1016/0892-6875(94)90114-7.
 Lewis, L.J., Jensen, P., and Barrat, J.L., 1997, Melting, freezing and coalescence of Au nanoclusters: *Physical Review B: Condensed Matter and Materials Physics*, v. 56, p. 2248–2257.
 Lewis, R.S., Ming, T., Wacker, J.F., Anders, E., and Steel, E., 1987, Interstellar diamonds in meteorites: *Nature*, v. 326, p. 160–162, doi: 10.1038/326160a0.
 McHale, J.M., Auroux, A., Perrotta, A.J., and Navrotsky, A., 1997, Surface energies and thermodynamic phase stability in nanocrystalline aluminas: *Science*, v. 277, p. 788–791, doi: 10.1126/science.277.5327.788.
 Mumin, A.H., Fleet, M.E., and Chrysosoulis, S.L., 1994, Gold mineralization in As-rich mesothermal gold ores of the Bogoso-Prestea mining district of the Ashanti Gold Belt, Ghana: Remobilization of “invisible” gold: *Mineralium Deposita*, v. 29, p. 445–460, doi: 10.1007/BF00193506.
 Navrotsky, A., 2001, Thermochemistry of nanomaterials: *Reviews in Mineralogy and Geochemistry*, v. 44, p. 73–103.
 Palenik, C.S., Utsunomiya, S., Reich, M., Kesler, S.E., Wang, L.M., and Ewing, R.C., 2004, “Invisible” Au revealed: Direct imaging of Au nanoparticles in a Carlin-type deposit: *American Mineralogist*, v. 89, p. 1359–1366.
 Reich, M., Kesler, S.E., Utsunomiya, S., Palenik, C.S., Chrysosoulis, S.L., and Ewing, R.C., 2005a, Solubility of Au in arsenian pyrite: *Geochimica et Cosmochimica Acta*, v. 69, p. 2781–2796, doi: 10.1016/j.gca.2005.01.011.
 Reich, M., Utsunomiya, S., Becker, U., Wang, L.M., and Ewing, R.C., 2005b, In-situ observation of thermodynamic size effects on melting of natural Au nanoparticles: *Geochimica et Cosmochimica Acta*, v. 69, p. 2781, doi: 10.1016/j.gca.2005.01.011.
 Saunders, J.A., 1990, Colloidal transport of gold and silica in epithermal precious-metal systems: Evidence from the Sleeper Deposit, Nevada: *Geology*, v. 18, p. 757–760, doi: 10.1130/0091-7613(1990)018<0757:CTOGAS>2.3.CO;2.
 Utsunomiya, S., and Ewing, R.C., 2003, Application of high-angle annular dark field scanning transmission electron microscopy, scanning transmission electron microscopy-energy dispersive X-ray spectrometry and energy-filtered transmission electron microscopy to the characterization of nanoparticles in the environment: *Environmental Science & Technology*, v. 37, p. 786–791, doi: 10.1021/es026053t.
 Waychunas, G.A., Kim, C.S., and Banfield, J.F., 2005, Nanoparticulate iron oxide minerals in soils and sediments: Unique properties and contaminant scavenging mechanisms: *Journal of Nanoparticle Research*, v. 7, p. 409–433.
 Zhang, H., Gilbert, B., Huang, F., and Banfield, J.F., 2003, Water-driven structure transformation in nanoparticles at room temperature: *Nature*, v. 424, p. 1025–1029.

Manuscript received 28 March 2006
 Revised manuscript received 5 July 2006
 Manuscript accepted 13 July 2006

Printed in USA